Biocatalytic, Stereoconvergent Alkylation of (*Z/E*)-Trisubstituted Silyl Enol Ethers

Runze Mao[†1], Doris Mia Taylor[†1], Daniel J. Wackelin[†1], Torben Rogge[‡2], Sophia J. Wu[1], Kathleen M. Sicinski[1], K. N. Houk[2], and Frances H. Arnold*[1]

[1]Division of Chemistry and Chemical Engineering, California Institute of Technology, Pasadena, California 91125, United States.

[2]Department of Chemistry and Biochemistry, University of California, Los Angeles, California 90095, United States.

[†]These authors contributed equally.

[‡] Present address: Institut für Chemie, Technische Universität Berlin, Strasse des 17. Juni 115, 10623 Berlin, Germany.

*Corresponding author. E-mail: frances@cheme.caltech.edu

Abstract: The selective conversion of mixtures of *Z/E* alkenes into chiral products is a synthetic challenge. Biocatalytic strategies can transform isomeric alkenes into stereopure compounds, but enzymes typically convert only one alkene isomer, thereby limiting the overall yield. Additional strategies have been used to interconvert alkene isomers, often at the cost of increasing energy consumption and chemical waste. Here, we present engineered hemoproteins derived from a bacterial cytochrome P450 that efficiently catalyze α-carbonyl alkylation of isomeric silyl enol ethers, producing stereopure products. Through screening and directed evolution, we generated $P450_{BM3}$ variant P411-SCA-5188, which catalyzes stereoconvergent carbene transfer in *Escherichia coli* with high efficiency and stereoselectivity to various *Z/E* mixtures of silyl enol ethers. In contrast to established *stereospecific* transformations that leave one isomer unreacted, P411-SCA-5188 converts both isomers to a stereopure product. This biocatalytic approach simplifies the synthesis of chiral α-branched ketones by eliminating the need for stoichiometric chiral auxiliaries, strongly basic alkali-metal enolates, and harsh conditions, delivering products with high efficiency and excellent chemo- and stereoselectivities.

Introduction

The use of enzymes to produce valuable fine chemicals, pharmaceuticals, and agrochemicals is at the forefront of the drive toward mild and ecologically sustainable synthesis techniques.[1-6] This can be largely attributed to the unparalleled chemo-, regio-, and stereoselectivities achievable through biotransformations.[5] Alkene biocatalytic functionalization, in particular, has garnered interest due to its potential to produce valuable chemicals from low-cost resources.[7] Enzyme-catalyzed alkene functionalizations offer advantages over their small molecule-catalyzed counterparts that include superior efficiency, unmatched selectivity, and the absence of toxic metals or reagents.[7-11] Nevertheless, enzymes often convert one alkene isomer while leaving the other unaltered (see a representative example in Figure 1A[12] among others[13]) or they catalyze the formation of distinct products based on the geometric properties of the alkenes.[14] Under certain conditions, enzymes may even display comparable conversion rates for both (*Z*)- and (*E*)-alkenes, resulting in the synthesis of identical products with inverse configurations (see a representative example in Figure 1B[15] among others[16]). Because the synthesis of geometrically pure alkenes can be very challenging, separation of the alkene isomers is often necessary to achieve high efficiency and stereoselectivity in biocatalytic processes.[17,18] To overcome this issue, in 2019 the Hartwig and Zhao groups pioneered a cooperative chemoenzymatic strategy for stereoconvergent reduction of *Z/E*-mixed alkenes that merges a photocatalytic cycle with an ene-reductase (Figure 1C).[19] Under blue light irradiation, the unreactive *Z* isomer could be converted to the active *E* isomer, which allowed an overall stereoconvergent reduction. This cooperative catalytic system is efficient and selective, but also requires additional inputs, such as blue-light irradiation and an expensive photocatalyst.

Arguably the most desirable transformation would use a stereoconvergent catalyst to directly convert a mixture of *Z/E* alkenes into a single product, with a theoretical yield of 100%. Although stereoconvergent catalysts have been studied extensively for small-molecule catalysis, stereoconvergent enzymes are seldom reported.[13,20-23] A stereoconvergent enzyme's active site must accommodate each stereoisomer, and in a unique pose, in order to have convergent selectivity toward a single product. In 2019, members of our group identified an engineered cytochrome P411 (a serine-ligated cytochrome P450 variant), designated P411$_{\text{Diane3}}$, that catalyzes the enantioconvergent intramolecular amination of racemic tertiary benzylic C(sp^3)–H bonds with sulfamoyl azides.[24] Very recently, the group also reported a diastereomer-differentiating enzyme, P411-INC-5186**,** which catalyzes the transformation of (*E*)-enol acetates to α-branched ketones with high levels of enantioselectivity, while simultaneously cyclopropanating the (*Z*)-enol acetates with excellent activities and selectivities (Figure 1D).[25] Although different products were generated from (*Z*)- and (*E*)-enol acetates, the β-carbons of the products of the (*Z*)- and (*E*)-enol acetates yielded an (*S*)-configured stereocenter. Inspired by this, we wondered whether this diastereomer-differentiating reaction could be directed toward a stereoconvergent biotransformation (Figure 1E).

We focused on the synthesis of α-branched ketones, a class of compounds prevalent in both natural and synthetic bioactive molecules.[26] From a synthetic perspective, stereoselective alkylation of alkali-metal enolates is widely employed for constructing α-branched ketone moieties.[26-28] Extensive studies have been conducted on controlling the stereochemistry of the α-carbon using various stoichiometric chiral auxiliaries and chiral catalysts.[28-30] The strong basicity of alkali-metal enolates, however, presents challenges in handling and limits the choice of functional groups. Additionally, the formation of distinct metal enolate isomers often complicates the stereochemical outcome of the subsequent reaction, as the product configuration is influenced by the geometry of the alkali-metal enolates. Furthermore, inherent difficulties in alkali-metal enolate alkylation, such as competitive *C*- and *O*-alkylation, overalkylation, and racemization, are non-trivial concerns.[28]

In this study, we showcase the adaptation and evolution of a biocatalytic platform initially designed for diastereomer-differentiating reactions to efficiently catalyze stereoconvergent alkylation. The evolved biocatalyst enables the enantioselective conversion of (*Z/E*)-mixed trisubstituted silyl enol ethers into chiral *α*-branched ketones. The biocatalytic method broadens the limited scope of enzymatic stereoconvergent transformations and complements traditional synthetic techniques, owing to its mild reaction conditions and excellent efficiency and selectivity.

Results and discussion

Initial screening and directed evolution of stereoconvergent alkyl transferase P411-SCA-5188.

We commenced this investigation by focusing on the coupling between a 1:1 *Z/E* mixture of butyrophenone-derived silyl enol ether **1a** and diazoacetonitrile **2a** (Figure 2). Silyl enol ethers serve as mild, stable enolate equivalents in comparison to alkali-metal enolates, offering ease of synthesis and handling. Compared to enol acetates previously used in P411-INC-5186-catalyzed cyclopropanation reactions,[25] silyl-protecting groups demonstrate increased propensity for hydrolysis, thereby promoting ketone product formation. Additionally, the inherent geometric information embedded in silyl enol ethers facilitates the development of the stereoconvergent capacity of the enzyme. Lastly, diazoacetonitrile **2a** was selected due to its potent electron-withdrawing nature, minimal steric interference, and the importance of the nitrile functional group.[32-33] We tested whether variants in the P411-INC-5186 directed evolution lineage could produce *α*-branched ketone **3a** through the coupling of **1a** and **2a**. Encouragingly, an evaluation of P411-INC-5186's precursors (Figure 2A, P411-INC-5183 to P411-INC-5186) indicated that all variants are capable of catalyzing the transfer of diazoacetonitrile **2a** to silyl enol ether **1a**, with an activity trend matching that of the cyclopropanation of enol acetates.[25] P411-INC-5186 demonstrated the highest activity and selectivity (200 TTN; 42% yield and 97% e.e. of **3a**, Figure 2A). When ethyl diazoacetate (EDA) was used as a carbene precursor, no alkylated product was detected (see Supplementary Table 1). Although P411-INC-5186 can catalyze this biotransformation with remarkable enantioselectivity, its activity required further improvement. Thus, we subjected P411-INC-5186 to sequential rounds of site-saturation mutagenesis (SSM) and screening, focusing on key active-site residues previously shown to affect carbene and nitrene transfer reactions.[34] Mutagenesis and screening introduced mutations V437A and L177M (Figures 2A, 2B and 2C), yielding variant P411-SCA-5188, which catalyzes the formation of **3a** with 290 TTN, 57% yield, and 99% e.e. (Figure 2A). Notably, the yield of alkylated product **3a** (57%) exceeded the proportion of either isomer in the 1:1 *Z/E* mixture of silyl enol ether **1a** (*Z*- and *E*-isomers constituting 50% each), strongly suggesting a stereoconvergent process. This biocatalytic stereoconvergence stands out from other reported olefin functionalizations, which predominantly adhere to stereospecific pathways.[12,14-16]

We next fine-tuned the reaction conditions to improve the yield (Figure 2A; see Supplementary Tables 5–8 for details). After examining various concentrations of *E. coli* harboring P411-SCA-5188 (OD_{600} values), concentrations of **1a** and **2a**, and pH values, we found that conducting the biotransformation using OD_{600} = 90, with 3 mM of **1a** and 37 mM of **2a** in M9-N aqueous buffer (pH 8) at room temperature afforded 85% yield with 99% e.e. (Figure 2A).

Experimental studies of stereoconvergent alkyl transferase P411-SCA-5188

To confirm that this biotransformation is in fact stereoconvergent, we obtained the isolated **1a** stereoisomers, (*Z*)-**1a** (99% stereopurity) and (*E*)-**1a** (94% stereopurity) and used them individually as substrates for P411-SCA-5188-catalyzed *α*-carbonyl alkylation with diazoacetonitrile **2a** (Figure 3A). Under standard conditions, P411-SCA-5188 converted pure (*Z*)-**1a** into **3a** with an *S* configuration in 49% yield (99 TTN) and 99% e.e. and transformed (*E*)-**1a** into **3a** with the same *S* configuration in 91% yield (230 TTN) and 99% e.e. (Figures 3A and 3B). Subsequently, we examined how catalytic efficiency against pure (*Z*)-**1a** and (*E*)-**1a** changed across the lineage (see Supplementary Tables 3 and 4 for more detail). Variants P411-INC-5183 to P411-INC-5185 exclusively catalyzed the transformation of (*Z*)-**1a** to **3a**, while leaving (*E*)-**1a** untouched. These results are consistent with the cyclopropanation of (*Z/E*)-trisubstituted enol acetates recently reported by the Arnold lab.[25] Upon introducing the W263M mutation, variants P411-INC-5186, P411-SCA-5187 and P411-SCA-5188 converted both (*Z*)-**1a** and (*E*)-**1a** into **3a**, accompanied by increases in activity

Since silyl enol ethers may degrade in the presence of water, forming butyrophenone **4a** after hydrolysis, we investigated whether butyrophenone **4a** could be converted to the *α*-branched ketone product **3a**. However, butyrophenone **4a** proved unreactive under standard conditions (Figure 3C), eliminating a potential conversion pathway from **4a** to **3a**. We then examined whether (*Z*)-**1a** and (*E*)-**1a** can possibly interconvert during the enzymatic process. Under standard conditions, but without **2a** and with a reduced reaction time of two hours to ensure sufficient residual **1a** for pre- and post-reaction stereopurity comparison, we observed no change in the stereopurity of *Z* or *E* isomers (Figures 3D and 3E).

Based on these findings and our previous computational studies on P411-INC-5186-catalyzed diastereomer-differentiating transformations,[25] we hypothesized the polar stepwise pathway for this alkylation depicted in Figure 3F. In this mechanism, diazoacetonitrile **2a** initially reacts with a hemoprotein to form electrophilic iron carbene **II**. The lone pair conjugation of the *β*-carbon of silyl enol ether **1a** endows it with nucleophilic characteristics, which facilitates the nucleophilic attack of (*Z*)-**1a** or (*E*)-**1a** onto **II**, resulting in the formation of intermediate (*Z*)-**III** or (*E*)-**III**. Crucially, during the attack of the *β*-carbon of either (*Z*)- or (*E*)-**1a** on **II**, the enzyme strictly controls the orientation of the ethyl group on the *β*-carbon of **1a** due to its proximity to the nucleophilic site and its more significant steric clash with electrophilic metal carbene **II** and surrounding residues. Consequently, regardless of whether (*Z*)- or (*E*)-**1a** is used as the substrate, the *β*-carbon on (*Z*)-**III** or (*E*)-**III** possesses the same *S* configuration, ensuring enantioconvergence at this carbon. Both intermediates (*Z*)-**III** or (*E*)-**III** are then enthalpically favored to undergo hydrolysis due to the unstable nature of these intermediates, yielding **3a**. Because the configuration of **3a** is determined in the initial nucleophilic attack step, the overall reaction is thus stereoconvergent.

Molecular dynamics simulations

To examine the mechanistic hypothesis further, molecular dynamics (MD) simulations were performed on intermediates (*E*)-**III** and (*Z*)-**III** in the active site of the enzyme. For (*E*)-**III**, both the cyano- and the ethyl-groups were found to orient towards the outward-facing side of the active site, with the CH_3-group of the ethyl-substituent angled in the direction of residue P329 (Figure 4A). In addition, the phenyl substituent is placed in a sterically accessible area at the top of the active site, defined by surrounding residues L75, M185, A264 and P329 (see also Supplementary Figures 5A and 6A for more details). The relatively bulky TMS group is preferentially oriented towards a non-congested area located at the backside of the active site in the vicinity of G268 and V328. Additionally, a rather short distance between the silyl ether oxygen and V328 indicates the presence of stabilizing C–H--O hydrogen bond interactions. With intermediate (*Z*)-**III**,

a comparable preferred orientation was observed, with the cyano and ethyl substituents again angled towards the front of the active site, allowing for the TMS and the phenyl substituent to be placed in the sterically accessible areas at the top and back of the active site, respectively (Figure 4B and Supplementary Figures 5B and 6B). In contrast, when the diastereomeric intermediate (*E*)-**IIIa**, which upon hydrolysis results in the formation of the minor enantiomer, was simulated, the large phenyl and TMS substituents are forced into less optimal positions (Figure 4C and Supplementary Figures 5C and 6C). In the preferred structure, the substrate's phenyl ring is placed in close proximity to A264, T438 and V328, resulting in a displacement of V328 and P329 and likely leading to a destabilization of (*E*)-**IIIa** (Supplementary Figures 5C and 6C). The significantly worse fit of (*E*)-**IIIa** in the active site is in good agreement with the experimental results and our mechanistic proposal. For the diastereomer of (*Z*)-**III**, (*Z*)-**IIIa**, the TMS group of the substrate was preferentially oriented towards the outward-facing side of the active site, with short distances between the TMS substituent and L75, T260 and A264 (Figure 4D and Supplementary Figures 5D and 6D). These short distances indicate unfavorable steric interactions and thus destabilization of this intermediate, reasonably resulting in the high enantioselectivity observed experimentally (Figure 3).

Substrate scope study

We next investigated the activity of P411-SCA-5188 on an array of *Z/E* mixtures of silyl enol ethers. Generally, P411-SCA-5188 catalyzes the alkylation of diverse *Z/E* mixtures of *α*-aryl, *β*-alkyl-substituted silyl enol ethers **1** with diazoacetonitrile **2a**, producing the desired products **3** in moderate to high yields and with exceptional enantioselectivities (up to 91% yield and >99% e.e., Table 1), regardless of the stereopurity of the silyl enol ethers employed. Substrates featuring various substituents on the *α*-aryl group exhibit excellent compatibility with this biotransformation. Electron-donating, -neutral, and -withdrawing substituents on the aromatic ring were all well-tolerated, generating *α*-branched ketones with consistently high enantioselectivity levels (**3a**–**3m**, Table 1). *Ortho*-, *para*- and *meta*-substituted *α*-aryl silyl enol ethers reacted efficiently with diazoacetonitrile **2a**, yielding the corresponding *α*-branched ketones (**3b**–**3i** and **3m**, Table 1). The introduction of a bulky group at the *para*-position also resulted in the *α*-branched ketone product with great enantioselectivity (95% e.e.), albeit with a reduced yield (**3d**, Table 1). Substrates containing a halogen functional group, such as fluoro- (**1e** and **1f**, Table 1), chloro- (**1g**), and bromo- (**1h**), proved viable for generating alkylated products (**3e**–**3h**, Table 1) with synthetically useful yields and excellent enantioselectivities. The incorporation of an electron-donating group also facilitated the synthesis of the *α*-branched ketone, yielding the desired product with over 99% e.e. (**3i**, Table 1). A structural variation made by replacing the aryl ring with thiophene (**1j**, Table 1) is also well-tolerated by the biocatalytic stereoconvergent transformation, generating **3j** in 88% yield and with 99% e.e. (Table 1). Moreover, *β*-substituents with diverse alkyl chains (**1k**–**1m**, Table 1) could be converted to the corresponding *α*-branched ketones in satisfactory yields and with high enantioselectivity. Notably, lengthening the *β*-alkyl chain appeared to have a detrimental effect on activity (**3k**, Table 1), likely due to steric clash of the alkyl chain with surrounding residues. Conversely, shortening the *β*-alkyl chain of the silyl enol ethers from propyl (**1k**, Table 1) or ethyl (**1a**, Table 1) to methyl (**1l**, Table 1) enhanced both activity and selectivity, resulting in a 91% yield and 99% e.e. for product **3l** (Table 1). Intrigued by this observation, we also examined the impact of the bulkiness of the silyl-protecting groups: reactivity was completely abolished when the trimethylsilyl group (TMS; **1a**, Table 1) was replaced with a triethylsilyl group (TES; **1n**, Table 1), a triisopropylsilyl group (TIPS; **1o**, Table 1), or a *tert*-butyldimethylsilyl group (TBDMS; **1p**, Table 1). We attributed this to the enhanced nucleophilicity and smaller steric hindrance provided by a TMS group, which allows the silyl enol ether to more effectively approach and interact with

its reaction partner in the enzyme pocket. Notably, the synthesis of trimethylsilyl enol ethers is more cost-effective compared to other silyl enol ethers.

Summary and Conclusions

We have developed an enzyme, $P450_{BM3}$ variant P411-SCA-5188, which catalyzes stereoconvergent alkylation of isomeric silyl enol ethers, yielding high-value chiral α-branched ketones. Compared to state-of-the-art methods for synthesizing chiral α-branched ketones from alkali-metal enolates, this work presents a streamlined, biocatalytic approach that operates under mild conditions. This strategy complements stereospecific biocatalytic alkene functionalization methods and more complex cooperative chemoenzymatic alkene functionalization approaches. We anticipate these findings will inspire further development of stereoconvergent enzymes to broaden the scope of biocatalysis and unlock biocatalytic strategies to address synthetic challenges.

Methods

Expression of P411-SCA variants

E. coli (*E. cloni* BL21(DE3)) cells carrying plasmid encoding the appropriate P411-SCA variant were grown overnight in 5 mL Luria-Bertani medium with 0.1 mg/mL ampicillin (LB_{amp}). Preculture (1 mL) was used to inoculate 50 mL of Hyperbroth medium with 0.1 mg/mL ampicillin (HB_{amp}) in an Erlenmeyer flask (125 mL). This culture was incubated at 37 ºC and 230 rpm for 2.5 hours. It was then cooled on ice for 30 min and induced with 0.5 mM isopropyl β-D-1-thiogalactopyranoside and 1.0 mM 5-aminolevulinic acid (final concentrations). Expression was conducted at 20 ºC, 150 rpm for 16–18 h. *E. coli* cells were then transferred to a conical centrifuge tube (50 mL) and pelleted by centrifugation (4,000*g*, 4 min, and 4 ºC). Supernatant was removed and the resulting cell pellet was resuspended in M9-N (pH = 8.0) buffer to OD_{600} = 30. An aliquot of this cell suspension (3–4 mL) was taken to determine protein concentration using the pyridine hemochromagen assay after lysis by sonication.

Stereoconvergent alkylation using whole *E. coli* cells harboring P411-SCA

Enzymatic reactions were set up in an anaerobic chamber. To a 2-mL vial were added the suspension of *E. coli* expressing P411-SCA (typically OD_{600} = 30, 360 µL), the silyl enol ether substrate (typically 3 µL of 400 mM stock solution in EtOH), and the diazoacetonitrile solution (typically 37 µL of 400 mM stock solution in EtOH). The final volume of the biotransformation was set to be 400 µL, with 10% vol EtOH. The reaction vial was then capped and shaken in the anaerobic chamber at room temperature and 600 rpm for 20 hours.

Data Availability

The original materials and data that support the findings of this study are available within the paper and its Supplementary Information or can be obtained from the corresponding author upon reasonable request.

Acknowledgments

Support by the National Science Foundation Division of Molecular and Cellular Biosciences (MCB-2016137 to F.H.A) is gratefully acknowledged. R.M. acknowledges support from the Swiss National Science Foundation (SNSF) Early Mobility Postdoctoral Fellowship (P2ELP2_195118). D.J.W. acknowledges support from the National Science Foundation Graduate Research Fellowship (DGE-1745301). K.M.S. acknowledges support from NIH Ruth L. Kirschstein National Research Service Award (1F32GM145123-01A1). Support by the National Science Foundation Division of Chemistry (CHE-2153972 to K.N.H.) and the Alexander von Humboldt-Foundation (Feodor Lynen Fellowship, T.R.) is gratefully acknowledged. We thank Dr. Scott C. Virgil for the maintenance of the Caltech Center for Catalysis and Chemical Synthesis (3CS). We thank Dr. Mona Shahgoli for mass spectrometry assistance. We thank Dr. David VanderVelde for the maintenance of the Caltech NMR facility. We also thank Dr. Sabine Brinkmann-Chen for the helpful discussions and comments on the manuscript. Calculations were performed on the Hoffman2 cluster at the University of California, Los Angeles.

Author Contributions Statement

R.M. conceptualized and designed the overall project under the guidance of F.H.A.. R.M. and D.J.W. carried out the initial screening of heme proteins. D.M.T. performed the directed evolution experiments, with support from S.J.W.. R.M. and D.J.W. investigated the substrate scope and reaction mechanism. K.M.S. purified and obtained both (*Z*)-**1a** and (*E*)-**1a**. T.R. carried out the computational studies with K.N.H providing guidance. R.M. and F.H.A wrote the manuscript with input from all authors.

Competing Interests Statement

The authors declare no competing interests.

Figure Legends/Captions

Figure 1. (A) Stereospecific biotransformation of *Z/E* alkene mixtures, exemplified by the asymmetric bioreduction by YersER from *Yersinia bercovieri*,[12] an ene-reductase from the Old Yellow Enzyme family, requires isomerically pure alkenes to achieve high yields. (B) Substrate-controlled biotransformation of *Z/E* alkene mixtures, exemplified by the asymmetric bioreduction by YqjM from *Bacillus subtilis*,[15] an ene-reductase from the Old Yellow Enzyme family, converts *Z* and *E* isomers into products exhibiting opposite configurations. (C) A cooperative chemoenzymatic system developed by the Hartwig and Zhao groups enables the effective stereoconvergent reduction of *Z/E* mixtures of alkenes. This method uses blue-light irradiation and a photocatalyst to convert the unreactive *Z* isomer to the active *E* isomer.[19] (D) A diastereomer-differentiating biotransformation method: carbene transferase P411-INC-5186 catalyzes the cyclopropanation of (*Z*)-enol acetates while simultaneously catalyzing (*E*)-enol acetates to *α*-branched ketones, both products containing an (*S*)-configured stereocenter. (E) This work: biocatalytic stereoconvergent alkylation of (*Z/E*)-trisubstituted silyl enol ethers to produce chiral *α*-branched ketones with high yields in a stereoconvergent manner. The structural illustration is adapted from Protein Data Bank (PDB) ID 5UCW (cytochrome $P450_{BM3}$ variant **E10**).[31] EWG, electron-withdrawing groups; R, organic groups; Ac, acetyl group; TMS, trimethylsilyl group.

Figure 2. Directed evolution for stereoconvergent alkylation. Reaction conditions: 2.5 mM **1a**, 37.5 mM **2a**, *E. coli* whole cells harboring P411 variants (OD_{600} = 30) in M9-N aqueous buffer (pH 8.0), 10% v/v

EtOH (co-solvent), room temperature, anaerobic conditions, 20 h. Optimized reaction conditions: 3 mM **1a**, 37 mM **2a**, *E. coli* whole cells harboring P411 variants (OD_{600} = 90) in M9-N aqueous buffer (pH 8.0), 10% v/v EtOH (co-solvent), room temperature, anaerobic conditions, 20 h. (A) Assessment of the enzyme lineage encompassing P411-INC-5186 and directed evolution culminating in P411-SCA-5188. Yields were calculated from HPLC calibration curves and the average of triplicate experiments (n = 3). (B) The mutated residues (N70, L177, W263, I327, and Q437) that enhance activity or enantioselectivity are highlighted in the active site of closely related P411 variant **E10** (PDB ID: 5UCW).[31] (C) Summary of beneficial mutations for stereoconvergent alkylation.

Figure 3. Mechanistic studies of stereoconvergent enzymatic alkylation. (A) and (B) Alkyl transfer reactions catalyzed by P411-SCA-5188 using (*Z*)- or (*E*)-**1a**. Reaction conditions: 3 mM (*Z*)-**1a** or (*E*)-**1a**, 37 mM **2a**, *E. coli* whole cells harboring P411-SCA-5188 (OD_{600} = 90) in M9-N aqueous buffer (pH 8.0), 10% v/v EtOH (co-solvent), room temperature, anaerobic conditions, 20 h. (C) Alkyl transfer reactions catalyzed by P411-SCA-5188 using butyrophenone **4a**. Reaction conditions: 3 mM butyrophenone **4a**, 37 mM **2a**, *E. coli* whole cells harboring P411-SCA-5188 (OD_{600} = 90) in M9-N aqueous buffer (pH 8.0), 10% v/v EtOH (co-solvent), room temperature, anaerobic conditions, 20 h. (D) and (E) Stereoretention of (*Z*)- or (*E*)-**1a**. Reaction conditions: 3 mM (*Z*)- or (*E*)-**1a**, *E. coli* whole cells harboring P411-SCA-5188 (OD_{600} = 90) in M9-N aqueous buffer (pH 8.0), 10% v/v EtOH (co-solvent), room temperature, anaerobic conditions, 2 h. (F) Proposed mechanistic pathway of P411-SCA-5188-catalyzed stereoconvergent alkylation. Yields were calculated from HPLC calibration curves and the average of triplicate experiments (n = 3). N.D. = not detected; TMS, trimethylsilyl group.

Figure 4. Molecular dynamics simulations. Representative structures of the most populated clusters obtained from MD simulations on (A) intermediate (*E*)-**III** and (B) intermediate (*Z*)-**III** and the corresponding diastereomers (C) (*E*)-**IIIa** and (D) (*Z*)-**IIIa**. Non-relevant, non-polar hydrogen atoms are omitted for clarity.

Table

Table 1. Substrate scope study. Reaction conditions: 3 mM **1**, 37 mM **2a**, *E. coli* whole cells harboring P411-SCA-5188 (OD_{600} = 90) in M9-N aqueous buffer (pH 8.0), 10% v/v EtOH (co-solvent), room temperature, anaerobic conditions, 20 h. Yields were calculated from HPLC calibration curves and the average of triplicate experiments (n = 3). Ar, aryl groups; Alkyl, alkyl groups; R, organic groups; TMS, trimethylsilyl group; TES, triethylsilyl group; TIPS, triisopropylsilyl group; TBDMS, *tert*-butyldimethylsilyl group; N.D. = not detected.

References

1 Straathof, A. J., Panke, S. & Schmid, A. The Production of Fine Chemicals by Biotransformations. *Curr. Opin. Biotechnol.* **13**, 548–556 (2002).

2 Schoemaker, H. E., Mink, D. & Wubbolts, M. G. Dispelling the Myths—Biocatalysis in Industrial Synthesis. *Science* **299**, 1694–1697 (2003).

3 Nestl, B. M., Nebel, B. A. & Hauer, B. Recent Progress in Industrial Biocatalysis. *Curr. Opin. Chem. Biol.* **15**, 187–193 (2011).

4 Wu, S., Snajdrova, R., Moore, J. C., Baldenius, K. & Bornscheuer, U. T. Biocatalysis: Enzymatic Synthesis for Industrial Applications. *Angew. Chem., Int. Ed.* **60**, 88–119 (2021).

5 Bell, E. L. *et al.* Biocatalysis. *Nat. Rev. Methods Primers* **1**, 46 (2021).

6 Patel, R. N. Biocatalysis for Synthesis of Pharmaceuticals. *Bioorg. Med. Chem.* **26**, 1252–1274 (2018).

7 Wu, S., Zhou, Y. & Li, Z. Biocatalytic Selective Functionalisation of Alkenes *via* Single-Step and One-Pot Multi-Step Reactions. *Chem. Commun.* **55**, 883–896 (2019).

8 McDonald, R. I., Liu, G. & Stahl, S. S. Palladium(II)-Catalyzed Alkene Functionalization *via* Nucleopalladation: Stereochemical Pathways and Enantioselective Catalytic Applications. *Chem. Rev.* **111**, 2981–3019 (2011).

9 Beller, M., Seayad, J., Tillack, A. & Jiao, H. Catalytic Markovnikov and *anti*-Markovnikov Functionalization of Alkenes and Alkynes: Recent Developments and Trends. *Angew. Chem., Int. Ed.* **43**, 3368–3398 (2004).

10 Rodriguez-Ruiz, V. *et al.* Recent Developments in Alkene Hydro-Functionalisation Promoted by Homogeneous Catalysts Based on Earth Abundant Elements: Formation of C–N, C–O and C–P Bond. *Dalton Trans.* **44**, 12029–12059 (2015).

11 Coombs, J. R. & Morken, J. P. Catalytic Enantioselective Functionalization of Unactivated Terminal Alkenes. *Angew. Chem., Int. Ed.* **55**, 2636–2649 (2016).

12 Yanto, Y. *et al.* Asymmetric Bioreduction of Alkenes Using Ene-Reductases YersER and KYE1 and Effects of Organic Solvents. *Org. Lett.* **13**, 2540–2543 (2011).

13 Yang, L.-C., Deng, H. & Renata, H. Recent Progress and Developments in Chemoenzymatic and Biocatalytic Dynamic Kinetic Resolution. *Org. Process Res. Dev.* **26**, 1925–1943 (2022).

14 Demming, R. M. *et al.* Asymmetric Enzymatic Hydration of Unactivated, Aliphatic Alkenes. *Angew. Chem., Int. Ed.* **58**, 173–177 (2019).

15 Stueckler, C. *et al.* Stereocomplementary Bioreduction of *α,β*-Unsaturated Dicarboxylic Acids and Dimethyl Esters using Enoate Reductases: Enzyme- and Substrate-Based Stereocontrol. *Org. Lett.* **9**, 5409–5411 (2007).

16 Wu, S. *et al.* Enantioselective *trans*-Dihydroxylation of Aryl Olefins by Cascade Biocatalysis with Recombinant *Escherichia coli* Coexpressing Monooxygenase and Epoxide Hydrolase. *ACS Catal.* **4**, 409–420 (2014).

17 Williams, J. M. J. *Preparation of Alkenes: A Practical Approach*. (Oxford University Press, Oxford, UK, 1996).

18 Nevesely, T., Wienhold, M., Molloy, J. J. & Gilmour, R. Advances in the *E – Z* Isomerization of Alkenes Using Small Molecule Photocatalysts. *Chem. Rev.* **122**, 2650–2694 (2022).

19 Litman, Z. C., Wang, Y., Zhao, H. & Hartwig, J. F. Cooperative Asymmetric Reactions Combining Photocatalysis and Enzymatic Catalysis. *Nature* **560**, 355–359 (2018).

20 Mohr, J. T., Moore, J. T. & Stoltz, B. M. Enantioconvergent Catalysis. *Beilstein J. Org. Chem.* **12**, 2038–2045 (2016).

21 Bhat, V., Welin, E. R., Guo, X. & Stoltz, B. M. Advances in Stereoconvergent Catalysis from 2005 to 2015: Transition-Metal-Mediated Stereoablative Reactions, Dynamic Kinetic Resolutions, and Dynamic Kinetic Asymmetric Transformations. *Chem. Rev.* **117**, 4528–4561 (2017).

22 Kroutil, W., Mischitz, M. & Faber, K. Deracemization of (±)-2,3-Disubstituted Oxiranes *via* Biocatalytic Hydrolysis Using Bacterial Epoxide Hydrolases: Kinetics of an Enantioconvergent Process. *J. Chem. Soc., Perkin Trans.* **1**, 3629–3636 (1997).
23 Chiappe, C. *et al.* Biocatalysis in Ionic Liquids: The Stereoconvergent Hydrolysis of *trans-β*-Methylstyrene Oxide Catalyzed by Soluble Epoxide Hydrolase. *J. Mol. Catal. B Enzym.* **27**, 243–248 (2004).
24 Yang, Y., Cho, I., Qi, X., Liu, P. & Arnold, F. H. An Enzymatic Platform for the Asymmetric Amination of Primary, Secondary and Tertiary C(sp^3)–H Bonds. *Nat. Chem.* **11**, 987–993 (2019).
25 Mao, R. *et al.* Enantio- and Diastereoenriched Enzymatic Synthesis of 1,2,3-Polysubstituted Cyclopropanes from (*Z/E*)-Trisubstituted Enol Acetates. *J. Am. Chem. Soc.* **145**, 16176–16185 (2023).
26 Carreira, E. M. & Kvaerno, L. *α-Functionalization of Enolates*. 3, 69–102 (WileyVCH, 2007).
27 Dugger, R. W., Ragan, J. A. & Ripin, D. H. B. Survey of GMP Bulk Reactions Run in a Research Facility between 1985 and 2002. *Org. Process Res. Dev.* **9**, 253–258 (2005).
28 Wright, T. B. & Evans, P. A. Catalytic Enantioselective Alkylation of Prochiral Enolates. *Chem. Rev.* **121**, 9196–9242 (2021).
29 Evans, D. A., Ennis, M. D. & Mathre, D. J. Asymmetric Alkylation Reactions of Chiral Imide Enolates. A Practical Approach to the Enantioselective Synthesis of *alpha*-Substituted Carboxylic Acid Derivatives. *J. Am. Chem. Soc.* **104**, 1737–1739 (1982).
30 Myers, A. G., Yang, B. H., Chen, H. & Gleason, J. L. Use of Pseudoephedrine as a Practical Chiral Auxiliary for Asymmetric Synthesis. *J. Am. Chem. Soc.* **116**, 9361–9362 (1994).
31 Prier, C. K., Zhang, R. K., Buller, A. R., Brinkmann-Chen, S. & Arnold, F. H. Enantioselective, Intermolecular Benzylic C–H Amination Catalysed by an Engineered Iron-Haem Enzyme. *Nat. Chem.* **9**, 629-634 (2017).
32 Sruthi, P. R. & Anas, S. An Overview of Synthetic Modification of Nitrile Group in Polymers and Applications. *J. Polym. Sci.* **58**, 1039–1061 (2020).
33 Wang, X. *et al.* Nitrile-Containing Pharmaceuticals: Target, Mechanism of Action, and Their SAR Studies. *RSC Med. Chem.* **12**, 1650–1671 (2021).
34 Yang, Y. & Arnold, F. H. Navigating the Unnatural Reaction Space: Directed Evolution of Heme Proteins for Selective Carbene and Nitrene Transfer. *Acc. Chem. Res.* **54**, 1209–1225 (2021).

Figure 1

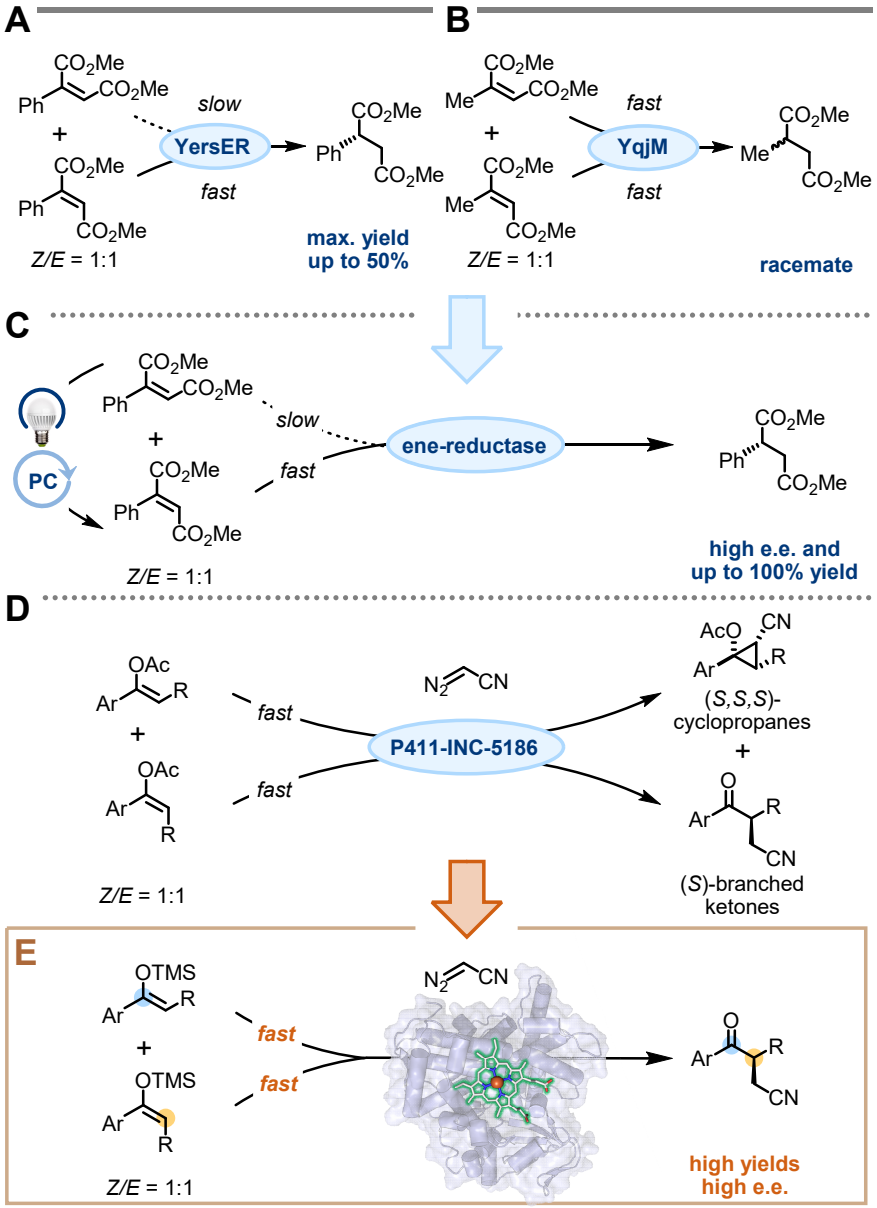
A
B
C
D
E
YersER
slow
fast
max. yield
up to 50%
Z/E = 1:1
YqjM
racemate
PC
ene-reductase
high e.e. and
up to 100% yield
P411-INC-5186
(S,S,S)-
cyclopropanes
(S)-branched
ketones
high yields
high e.e.

Figure 2

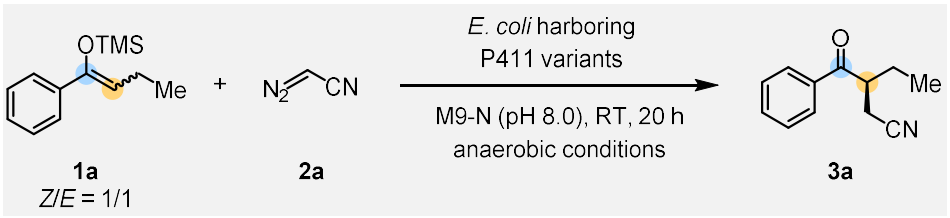
OTMS
Me
+
N2
CN
E. coli harboring
P411 variants
M9-N (pH 8.0), RT, 20 h
anaerobic conditions
O
Me
CN
1a
Z/E = 1/1
2a
3a

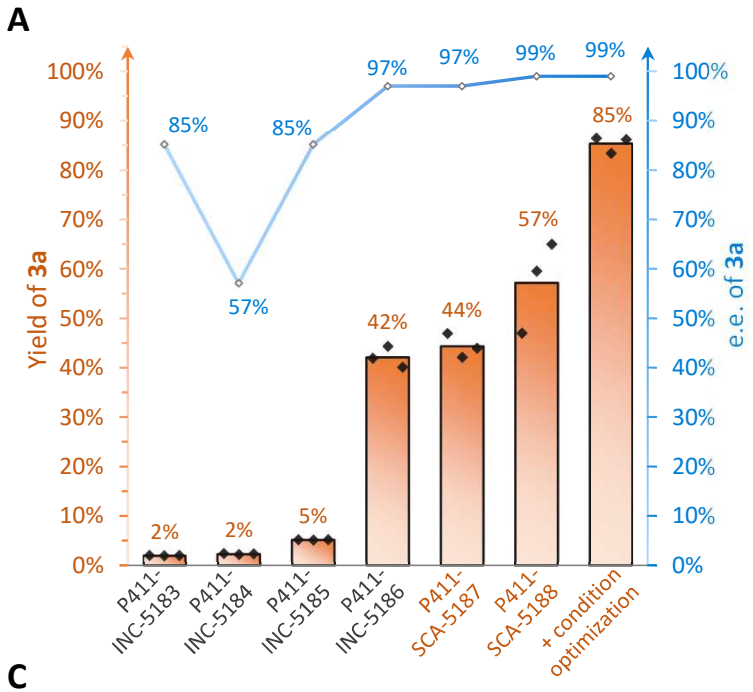
A
Yield of 3a
e.e. of 3a
100%
90%
80%
70%
60%
50%
40%
30%
20%
10%
0%
85%
57%
85%
97%
97%
99%
99%
2%
2%
5%
42%
44%
57%
85%
P411-INC-5183
P411-INC-5184
P411-INC-5185
P411-INC-5186
P411-SCA-5187
P411-SCA-5188
+ condition optimization

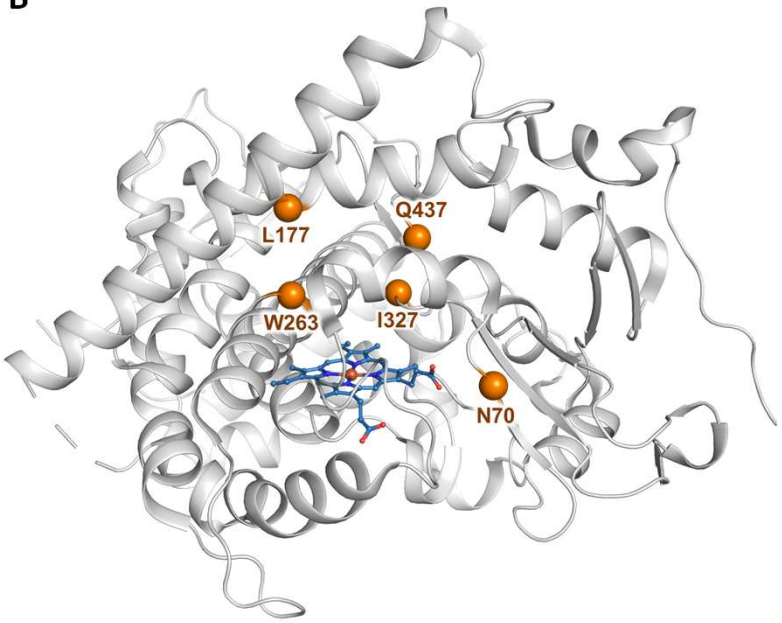
B
L177
Q437
W263
I327
N70

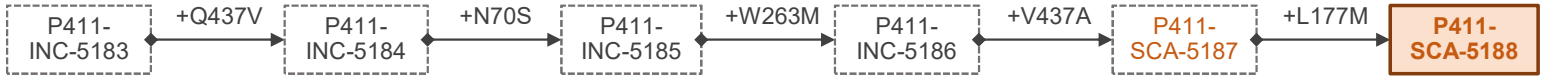
C
P411-INC-5183
+Q437V
P411-INC-5184
+N70S
P411-INC-5185
+W263M
P411-INC-5186
+V437A
P411-SCA-5187
+L177M
P411-SCA-5188

Figure 3

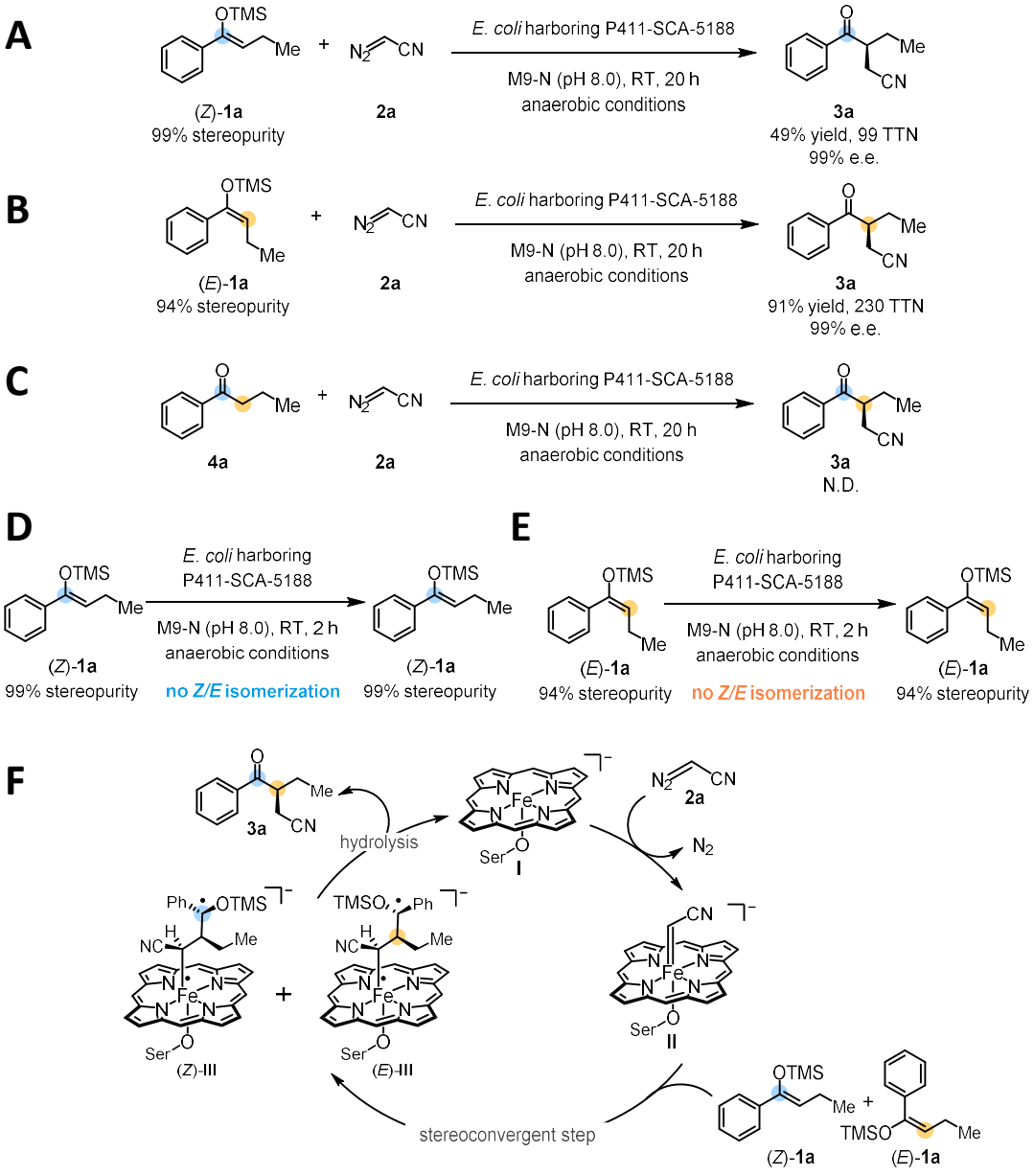
A
OTMS
Me
(Z)-1a
99% stereopurity
2a
E. coli harboring P411-SCA-5188
M9-N (pH 8.0), RT, 20 h
anaerobic conditions
3a
49% yield, 99 TTN
99% e.e.
B
(E)-1a
94% stereopurity
91% yield, 230 TTN
99% e.e.
C
4a
N.D.
D
no Z/E isomerization
E
F
hydrolysis
stereoconvergent step
(Z)-III
(E)-III

Figure 4

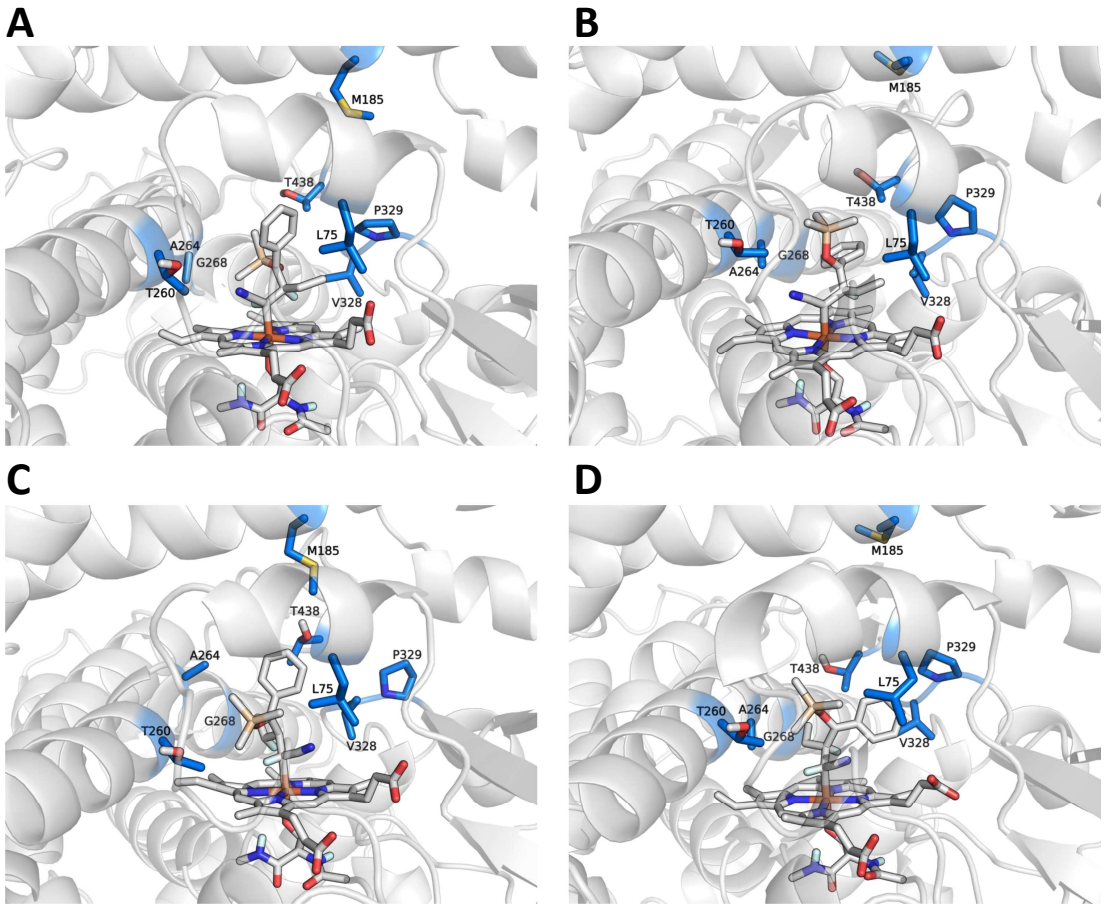
A
M185
T438
P329
L75
A264
G268
T260
V328
B
M185
T438
P329
T260
L75
G268
A264
V328
C
M185
T438
A264
P329
L75
G268
T260
V328
D
M185
P329
T438
L75
T260
A264
G268
V328

Table 1

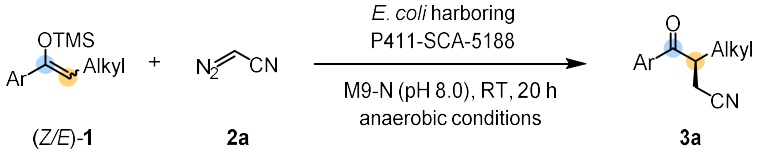

(*Z*/*E*)-**1** **2a** **3a**

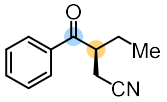

3a
85% yield,
190 TTN, 99% e.e.

from *Z*/*E* (1/1) **1a**

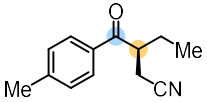

3b
43% yield,
86 TTN, 97% e.e.

from *Z*/*E* (1/2.2) **1b**

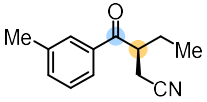

3c
59% yield,
120 TTN, 97% e.e.

from *Z*/*E* (1/1.7) **1c**

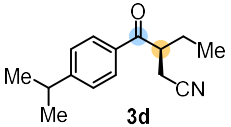

3d
8% yield,
18 TTN, 95% e.e.

from *Z*/*E* (1/2.3) **1d**

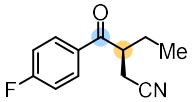

3e
76% yield,
170 TTN, 93% e.e.

from *Z*/*E* (1/1.2) **1e**

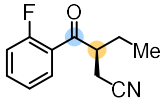

3f
32% yield,
73 TTN, 99% e.e.

from *Z*/*E* (1/0.1) **1f**

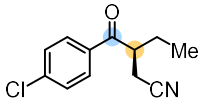

3g
11% yield,
21 TTN, 90% e.e.

from *Z*/*E* (1/0.5) **1g**

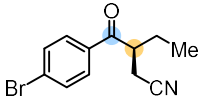

3h
38% yield,
86 TTN, >99% e.e.

from *Z*/*E* (1/0.05) **1h**

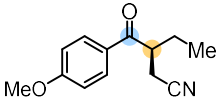

3i
57% yield,
130 TTN, >99% e.e.

from *Z*/*E* (1/1) **1i**

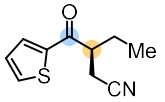

3j
88% yield,
200 TTN, >99% e.e.

from *Z*/*E* (1/0.6) **1j**

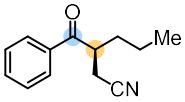

3k
18% yield,
37 TTN, 91% e.e.

from *Z*/*E* (1/1.5) **1k**

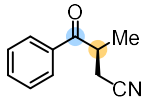

3l
91% yield,
210 TTN, 99% e.e.

from *Z*/*E* (1/1) **1l**

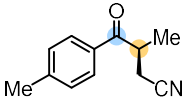

3m
69% yield,
150 TTN, 90% e.e.

from *Z*/*E* (1/2.3) **1m**

1n, R = TES
1o, R = TIPS
1p, R = TBDMS

3a, N.D.